Eur Radiol (2005) 15: 1881–1887
DOI 10.1007/s00330-005-2741-x

Amina Abdelmoumene
Patrick Chevallier
Marc Chalaron
Frédéric Schneider
Francis R. Verdun
Phillipe Frascarolo
Reto Meuli
Pierre Schnyder
Alban Denys

Detection of liver metastases under 2 cm: comparison of different acquisition protocols in four row multidetector-CT (MDCT)

Received: 2 August 2004
Revised: 21 February 2005
Accepted: 2 March 2005
Published online: 3 May 2005

A. Abdelmoumene (✉) · P. Chevallier · M. Chalaron · F. Schneider · R. Meuli · P. Schnyder · A. Denys
Department of Diagnostic and Interventional Radiology,
University Hospital Centre (CHUV),
1011 Lausanne, Switzerland
e-mail: ninaabdelmoumene@hotmail.com
Tel.: +41-21-3144470
Fax: +41-21-3144443

F. R. Verdun
University Institute for Applied Radiophysics, Grand-Pré 1,
1007 Lausanne, Switzerland

P. Frascarolo
Department of Anaesthesiology,
University Hospital Centre (CHUV),
1011 Lausanne, Switzerland

Abstract This study compared different acquisition protocols performance to detect small liver metastases (<2 cm). Thirty consecutive patients with histologically proven hepatic metastases were explored by MDCT at the liver equilibrium phase by four successive acquisitions. We compared the following protocols (1–4): 5/30/1.5 (section thickness/table speed/pitch); 5/15/0.75; 5/11.25/0.75; and 2.5/15/1.5 with the same X-ray dose. The gold standard was based on patient radiological follow-up. Evolutive lesions were considered as true positive (TP). The described lesions, not found on the follow-up exams despite tumoral progression, were considered as false positive (FP). Stable lesions could not be considered as metastasis and were eliminated. One hundred and seventy-six lesions were detected: 61 TP and 91 FP. Twenty-four lesions were eliminated. The mean kappa values for protocols 1, 2, 3 and 4 were, respectively, 0.43, 0.68, 0.73 and 0.51 (0.61–0.80: substantial agreement) and the mean areas under the ROC curve were, respectively, 0.76, 0.87, 0.86 and 0.80. The results of protocols 2 and 3 were significantly superior to those of protocols 1 and 4. MDCT protocols using thin sections or an increased table speed are less efficient in detecting small metastases.

Keywords Multidetector row · Liver metastases · Computed tomography

Introduction

Liver metastases detection is crucial for determining the best treatment option and improve patient outcome [1]. In patients with GI cancer and other selected malignancies, performing partial hepatic resection showed increasing survival [2, 3]. Accurate detection as well as determination of the segmental localisation and the size of all hepatic lesions are required to assess surgical resectability or response to chemotherapic treatment. Contrast-enhanced helical CT is the recommended modality for preoperative detection and assessment of resectability of liver metastases [4–7]. However, with helical CT, detection of liver metastases smaller than 1 cm has been demonstrated to be poor, with a sensitivity of 56% [8]. Introduction of multidetector CT has allowed faster scanning of large volumes using thin sections. The entire liver can be rapidly imaged using thin collimation during a single breath-hold after contrast material enhancement for all patients. This requires the development of new imaging protocols to obtain the best compromise between X-ray dose, contrast-to-noise ratio, partial volume effect and acquisition time for the detection of small low contrast lesions [9, 10]. Thinner collimation should improve lesion detection as partial volume effect is reduced. However, an experimental study comparing a four detector row CT with a single detector CT for

the detection of low contrast lesion by using a phantom, has demonstrated that reduction of slice thickness requires a significant increase of radiation dose to achieve an acceptable CNR with MDCT as compared with single slice CT [11]. From the same experimental study, slice thickness of 5 mm offered the best compromise between CNR and dose. Thinner slices (2.5 mm) required a much higher X-ray dose to achieve similar CNR. However, because of its experimental design, this study did not take into account partial volume effect and was focused on lesions with a very low contrast (8 Hounsfield units).

Furthermore, in clinical practice, partial volume effect may be a critical issue if contrast between liver and tumoral lesions is low, in particular for hypovascular lesions. For these latter reasons, we designed this clinical study in order to compare four protocols with MSCT and to determine the optimal CT protocol for detection of hepatic metastases.

Materials and methods

Patient population

Thirty consecutive patients (12 men and 18 women; age range, 36–83 years; mean age, 59.4 years) who had histologically proven hepatic metastases were prospectively enrolled in this study. The primary tumor originated in the following sites: colon (n=17), rectum (n=4), and breast (n=9). Institutional Review Board approval was granted and informed consent was obtained from each patient.

CT imaging protocol

CT scans were performed with a multidetector row CT system (Light speed QX/i, GE Medical Systems; version 3.1; Milwaukee, Wisc., USA). Before injection of contrast material, images were obtained through the entire liver, at 5 mm collimation during a single breath-hold. The scanning location was determined by mean of the scout digital radiography. The technical parameters used were 120 kV, 220 mA, rotation speed of 0.8 s, table speed of 11.25 mm per gantry rotation, pitch of 0.75, and field of view of 30–40 cm. The filter used was the standard filter for abdominal examination.

After this non-enhanced CT scanning, all patients received a low-osmolarity contrast medium of Iopental [Imagopaque 300 R (300 mg I/mP); Nycomed, Munich, Germany]. A volume of 1.5 ml/kg body weight was administered by means of a power injector (Tomojet winjet 3.1-Bruker AG) at rate of 3 ml/s through a 20 G plastic IV catheter placed in an antecubital vein.

The routine imaging oncologic protocol was then performed, involving the examination of the chest at the arterial phase (25 s delay post-injection) and the abdominal and pelvic regions at the venous phase (60-s delay post-injection), with the following parameters settings: 120 kV, 220 mA, rotation speed of 0.8 s and table speed of 11.25 mm per gantry rotation, pitch 0.75.

The images of the non-enhanced scan allowed the radiologist to determine the best scanning location on the z-axis, covering a distance of 7.5 cm, containing the maximum of small hepatic lesions that would be explored by our four acquisitions protocols used in this study. For the purpose of the study, we performed four successive acquisition at the equilibrium phase of the liver, 120 s delay after contrast medium injection, in a single breath-hold. To minimize bias due to contrast material dynamics, the four acquisitions were performed at the equilibrium phase in random order.

The following sets of acquisitions were used:

- For set 1:5 mm elementary collimation, 5 mm reconstructed slice thickness, table speed: 30 mm per rotation, rotation speed 0.8 s and pitch of 1.5, 120 kV and 440 mA were used.
- For set 2:5 mm elementary collimation, 5 mm reconstructed slice thickness, table speed: 15 mm per rotation, rotation speed 0.8 s and pitch of 0.75, 120 kV and 220 mA were used.
- For set 3:3.75 mm elementary collimation, 5 mm reconstructed slice thickness, table speed: 11.25 mm per rotation, rotation speed 0.8 s and pitch of 0.75, 120 kV and 220 mA were used.
- For set 4:2.5 mm elementary collimation, 2.5 mm reconstructed slice thickness, table speed: 15 mm per rotation, rotation speed 0.8 s and pitch of 1.5, 120 kV and 440 mA were used.

We used the International Electrotechnical Committee Standard definition of pitch corresponding to the ratio of table advancement to the irradiated width per 360° tube rotation. X-ray dose delivered for each set of acquisition was identical, with a dose-length product (DLP) equal to 176 mGy cm for the four protocols. The weighted CT dose index (CTDIw) was equal to 0.1 mGy/mAs for each acquisition protocol. To give practical X-ray dose information, the DLP corresponding to an acquisition of 7.5 cm length was converted in effective dose for each acquisition protocol using the conversion factor that has to be applied when scanning the upper part of the abdomen (i.e. 0.015 mSv/mGy cm [7]). The effective dose was equal to 3 mSv for each acquisition protocol. The total acquisition time of the four sets was 19.1 s and was accomplished in a single breath-hold. Acquisition times for protocols 1–4 were, respectively, 2.8, 5.2, 6.4 and 4.7 s. The follow-up CT scans were performed according to routine practice.

Images interpretation and analysis

Out of 30 patients, only patients with a follow-up demonstrating tumor progression in the liver were kept for

the study. Tumor progression was defined according to RECIST criteria and corresponds to at least a 20% increase in the sum of the longest diameter of target lesions [12].

Twenty-two patients constituted the final study group (10 men and 12 women with a mean age of 62.6 years). The primary tumor originated in the following sites: colon (n=12), rectum (n=4), breast (n=6). They all had a radiological follow-up longer than 3 months in our institution (median: 13.4 months, range: 5–18 months), which was part of the routine oncologic follow-up.

Six patients received chemotherapy during the follow-up period and 16 patients were under therapeutic window. Images of the four acquisition protocols were displayed on hard copy with 4×5 images format and the same window level of 150 and window width of 80, which were appropriate for representation of the liver parenchyma.

Patient information and technical parameters were masked on the films. Only lesions of 2 cm diameter or smaller were analyzed. Lesions exceeding 2 cm had been crossed on each film and the hepatic segmentation according to the Couinaud numbering system was drawn directly on every film by one radiologist before the readings in order to prevent mislocation of the lesions by the readers.

Three sets of images obtained for each of the four acquisition protocols were placed in individual folders; this represented a total of 264 readings for all patients. The examinations were reviewed independently by three radiologists (P.C., M.C., F.S.): two senior radiologists with extensive and comparable experience in liver CT imaging of more than 10 years (reader 1 and 2) and one junior radiologist, 2nd year fellow in general radiology (reader 3). The three readers underwent a training session in which the protocol was presented and explained using films of patients excluded for missing follow-up. How to number lesions and how to fill the study forms was detailed.

The radiologists knew that patients were at risk of hepatic metastasis and were referred for routine CT follow-up exam, but did not have any other information about the medical history of the patients. The reading procedure was performed in four sessions at 3-week intervals. At each session, images obtained by one individual acquisition protocol per patient were reviewed so that each patient was presented only once during each session, and the four protocols were equally represented. To limit learning bias, the patient's films appeared in random order in each reading session. At the time of interpretation, the readers were blinded to the results of other imaging protocols and to the results of the other observers. They were asked to number on the film each identified lesion and to mark on the form its segmental location and its size. A confidence level was assigned for the visibility of the lesions: level 4, lesion certainly visible (100% certain); level 3, lesion probably visible (75% certain); level 2, lesion possibly visible (50% certain), and level 1, lesion hardly visible (25% certain).

After completion of all blinded review sessions, two radiologists (A.D., A.A.) who were not involved in the images interpretation reviewed in consensus all the films for each patient. During this session, corresponding lesions were matched in between different acquisitions and readers for statistical evaluation.

The lesions that revealed an increase in size on follow-up exams were considered as metastases with certainty and true positive (TP). The lesions that were not found on follow-up exams, despite the fact that patients presented radiological progression of other lesions in the liver, were considered as false positive (FP). Lesions that showed stability in size on the follow-up CT scans were eliminated from the study, since they could not be considered as metastasis with certainty [13, 14].

Statistical methods

To assess inter-observer variability, we calculated the kappa statistic for multiple observers, by using the non-weighted binary Kappa statistic for the four acquisition protocols. A kappa value of 0.01–0.2 was considered slight agreement; 0.21–0.4, fair agreement; 0.41–0.60, moderate agreement; 0.61–0.80, substantial agreement; and 0.81–1.00, almost perfect agreement.

For each acquisition protocol, the receiving operating characteristic curve was filled to each observer's confidence rating data base, using a maximum likelihood estimation. The diagnostic accuracy of each acquisition protocol for each observer and each acquisition was estimated by calculating the area under the receiver operating characteristic curve (Az index). Composite ROC curves representing the performances of all the readers as a single one were obtained for each acquisition protocol by using the maximum likelihood curve fitting algorithm to rate the pool data of the three readers. Differences between acquisitions protocols in terms of mean Az values were analyzed statistically using the two-tailed Student t-test for paired data; a two-tailed P-value <0.05 was considered significant. The statistical package used was JMP (version 5.0.1; SAS Institute, Cary, N.C., USA).

Results

A total of 176 liver lesions were visualised, 61 TP and 91 FP, in 22 patients. Twenty-four lesions were eliminated because they could not be considered as metastases with certainty on follow-up exams.

Mean lesion size was 8.8 mm with a range of 2 mm to 2 cm. Mean lesion size of TP lesions was 9.8 mm and mean lesion size of FP lesions was 8 mm. The mean appa values of the three observers for each acquisition were 0.43 for protocol 1; 0.68 for protocol 2; 0.73 for protocol 3 and 0.51 for protocol 4. This indicates a moderate agreement between readers for the protocols 1 and 4; and a substantial agreement between the readers for protocols 2 and 3. Re-

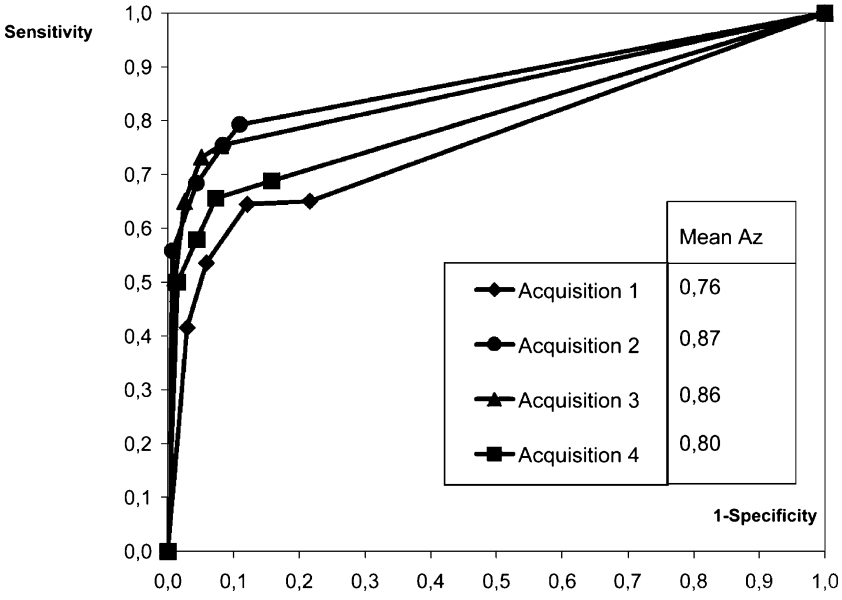

Fig. 1 ROC curves for the four acquisition protocols

ceiver operating characteristic curves constructed on the basis of pooled data from all the readers for each protocol are shown in Fig. 1. The mean Az values for the protocols 1, 2, 3 and 4 were, respectively, 0.76, 0.87, 0.86 and 0.80.

Areas under the ROC curves were always greater than 0.7, showing good diagnosis accuracy for the four imaging protocols. However, areas under the ROC curves were higher for the protocols 2 and 3 with a statistically significant difference compared to the protocols 1 and 4.

Discussion

CT scan has proved to be an excellent and widely used modality for the detection and preoperative assessment of hepatic tumors [6, 15, 16]. Detection of small hepatic metastases under 2 cm in diameter remains a challenge with multidetector row CT despite an increased spatial and temporal resolution. These advances in technology called for the development of optimized acquisition protocols, but there is no agreement in the literature on the optimal collimation and pitch for detection of small hepatic lesions using MDCT. First results of studies performed with SSCT have shown that portal-phase contrast-enhanced helical CT is extremely sensitive (91%) in detecting hepatic lesions greater than 1 cm, but is insensitive below this diameter (56%) [8].

With the use of multidetector row CT, different acquisition protocols are available to produce a particular reconstructed section thickness. In our study, we compared four protocols with different slice thickness (5 mm reconstructed slice thickness with elementary collimation of 5 and 3.75 mm versus 2.5 mm reconstructed slice thickness with 2.5 mm elementary collimation) and same slice thickness of 5 mm (with elementary collimation of 5 and 3.75 mm) with three different table speeds (30, 15 and 11.25 mm per rotation), (Fig. 2). As we wanted to specifically evaluate the influence of slice thickness and table speed on the detection of low contrast lesions, we used the same radiation dose for the four protocols. The CTDIw applied was adapted to the recommended dose for abdominal CT by the European Guidelines, which suggest CTDIvol values ranging from 17.5 to 29.5 mGy for liver screening investigation [17–21]. In addition, in a previous experimental study performed with a phantom simulating the X-ray absorption of a standard abdomen, it has been demonstrated that for the detection of 5 mm lesions to achieve a CNR of 1, which ensures a detection rate of 100%, the X-ray dose required correspond to a CTDIw=20 mGy [11]. Thus, we determined the acquisition parameters (tube current setting) in order to obtain a CTDIw=23 mGy for all the protocols tested. We would expect that reducing partial volume effect by scanning with thinner sections would lead to improved sensitivity in the detection of small liver metastases. However, in our study 5 mm slice thickness proved to be more efficient in detection of small lesion than 2.5 mm slice thickness, for the same irradiation of the patient. Imaging the liver with 2.5 mm slice thickness resulted in more noisy images with significantly lower performance in the detection of hepatic lesions as previously demonstrated experimentally. Image noise measurement was not performed in our study. In the fantom by Hu et al., using the same CT scanner as in the present study, the lowest noise-ratio 4-slice CT/conventional CT was achieved with 2.5 mm beam collimation and pitch of 0.75, and the highest with 2.5 mm beam collimation and pitch of 1.5 (section thickness in both 5 mm) [22]. The ability to detect a focal liver lesion depends on the contrast between the lesion and the

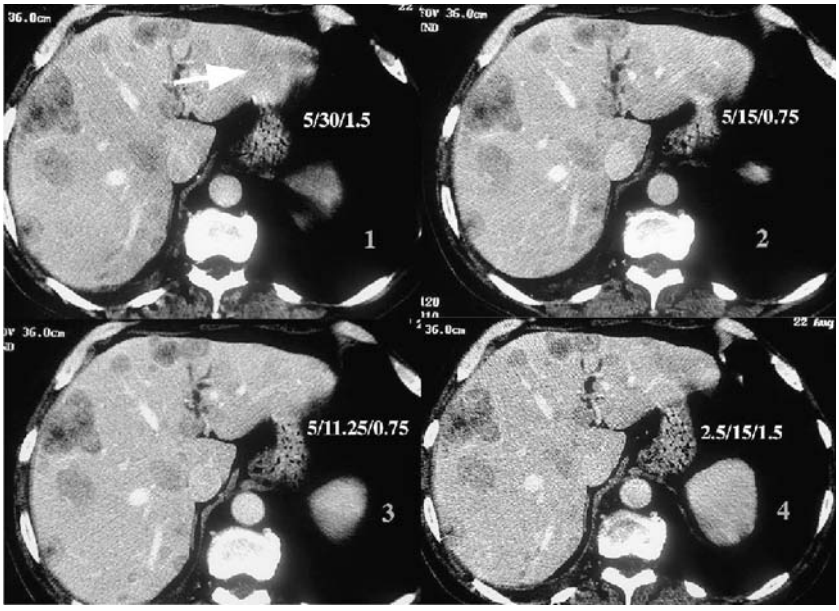

Fig. 2 Slices obtained at the same level for protocols 1, 2, 3 and 4. Artefacts in the left lobe are observed in protocol 1 (*arrow*). Images of protocol 2 and 3 produced similar quality in particular for the detection of lesions in segment 7 that are hardly visible in protocol 4 images

liver and on the noise corresponding to the contrast-to-noise ratio (CNR). Therefore, an increase in noise level decreases the ability to detect low contrast lesions. In CT, the noise depends on the total number of photons used to produce the image, which is function of the selected milliamperes–seconds. In general, the higher the radiation dose the lower the image noise is. These results of our study are in good agreement with the experimental results of Verdun et al. They demonstrated that using an elementary collimation of 2.5 mm and 2.5 mm reconstructed slices thickness with a pitch of 1.5 with the same CT scan, those parameters corresponding to the acquisition protocol 4 in the present study, does not permit achievement of a CNR value of 1, whatever the X-ray dose, while with significant increase of X-ray dose an acceptable CNR of 0.6 could be obtained. A CNR of 1 was necessary to achieve a 100% detection rate of 5 mm lesions, and a CNR of 0.6 to achieve a 100% detection rate of 9 mm lesions. [11]. The lower efficiency of thinner sections in detecting small hepatic lesions may be attributed to the geometric efficiency of the detectors that deteriorates with thin collimation [11]. Indeed, the penumbral region of the X-ray beam which was fully used by single detector CT is excluded with MDCT and only the ombra is directed to the active area of the detector. This effect is most prominent with our MDCT at thin slices and requires an increase in dose. This dose increase requirement depends on the implementation of beam collimation and image interpolation algorithms and varies between scanner manufacturers [23].

Another reason for the need to increase the X-ray dose when dealing with thin sections with MDCT may be related to the improvement in longitudinal resolution, allowing better control of the SSP compared with single detector row CT but at the price of dose. In the literature, Weg et al. in 1998, first answered the question whether thinner section thickness really improved lesion detection by using a dual-detector scanner with 2.5 mm elementary collimation thickness and compared reconstructed sections of 2.5, 5, 7.5 and 10 mm. They demonstrated that the use of 2.5 mm thick sections resulted in an 18% increase in detection rate of lesions versus 5 mm reconstructed thick sections for small lesions and observed that lesion conspicuity and radiologist confidence in lesion detection increased as section thickness decreased [24]. However, detector geometry of this unit is completely different from four row multidetector CT and this may account for the differences with our study. In our study, we did not evaluate the protocol 2.5 mm elementary collimation and 5 mm reconstructed sections thickness, pitch of 1.5. However, the experimental study of Verdun et al. shows that this protocol is more efficient in term of X-ray dose than the use of elementary collimation of 5 mm [11]. Furthermore, they postulated that a better CNR should be achieved with an elementary collimation of 2.5 mm instead of 5 mm for a reconstructed section of 5 mm because of the production of a higher amplitude of the impulse response with an elementary collimation of 2.5 mm [11, 25].

Haider et al., using a four detector row helical system from GE, performed a single acquisition with the following parameters: 120 kV, 230–330 mA, table speed: 7.5 mm/rotation, HS mode and pitch of 3 at the portal phase. They then compared reconstructed images at collimation of 5, 3.75 and 2.5 mm with 50% overlap. They did not obtain an improved sensitivity in the detection of small hepatic metastases with reconstructed images at collimation less than 5 mm [26]. When we used 5 mm reconstructed slice thickness, we observed that similar results were obtained with table speed of 15 mm per rotation and 11.25 mm per rotation while the results were poor with table speed of 30

mm per rotation. This can be explained by a widening of the section sensitivity profile (SSP) while dealing with a pitch value greater than 1. Thus, for 5 mm beam collimation with table speed of 30 mm per rotation, the FWHM was 6.4 mm corresponding to a widening of slice thickness equal to 20%, resulting in an increase of partial volume effect [22, 27].

In addition, there is a 10% increase in noise ratio when increasing the table speed from 15 to 30 mm per rotation, this also contributes to reduce the CNR [22]. We observed that images obtained with protocol 1 using a pitch value of 1.5 with an increase in acquisition speed (table speed: 30 mm) produced artifacts, mainly on the posterior sector of the right lobe and on the periphery of the left lobe (Fig. 2). These artifacts induced by the vertebrae, the ribs and the air in the stomach may also account for the lower detection rate of small metastases. Artefacts associated with spiral CT are reported in the literature, and Witling and Timmer demonstrated on cadaver studies that the artefacts increased with increased table speed and that they were less severe when the pitch is reduced [28, 29]. Comparing protocols 2 and 3 did not reveal a significant difference in the detection of small hepatic lesions. We would have expected better results with 3.75 mm elementary collimation than with 5 mm elementary collimation, taking into account the *z*-filtering reconstruction which acts as low pass filter on the image noise. In an experimental study, Verdun et al. demonstrated that 3.75 mm elementary collimation with a pitch of 0.75 offers the best compromise between dose and CNR when the reconstructed section is 5 mm [11]. In our clinical study, this protocol showed similar results as protocol 2, perhaps this could be attributed to the difference of "background", which is less homogeneous in clinical practice due to "structured noise" or "anatomical noise". Although similar results were obtained with protocol 2 and 3, we would however recommend to use protocol 2) when acquisition time is a critical issue, for instance when two arterial phases are performed, or with patients presenting limited apnea. When acquisition time may be increased we prefer to use the protocol 3. First, it allows reconstruction of thinner sections, and second, it offers a better CNR.

In addition, the routine use of thicker slices compared to thinner slices for detection of small liver metastasis offers advantages in terms of radiologist productivity and in terms of operating costs such as filming printing or PACS archiving.

Study limitations

The major limitation of our study resides in the absence of pathologic or surgical assessment of the lesions. We dealt with this limitation first by keeping in our final study group only patients with a radiological follow-up showing a tumoral progression in the liver and second by eliminating lesions that could not be considered as metastases with certainty on the follow-up exams [13, 14]. Longer patient follow-up may have revealed that there were metastases among these eliminated lesions.

This study includes only a small number of patients. However, we believe that our results are valid because this study includes a fairly large number of lesions and the reproductibility of the method is good as demonstrated by the kappa statistic for the results of the different readers. Perhaps that a larger population would have shown a different result between protocol 2 and protocol 3.

In our study, for methodologic reasons,we choose to assess specifically the effect of slice thickness and table speed on detection of low-contrast lesion. Therefore, we applied an identical radiation dose which was adapted to respond to European guidelines for liver screening investigation, but in clinical practice, the benefit of thinner sections could be realized by minimizing image noise with an increase in radiation dose. Our study was performed with the MDCT Lightspeed from GE Medical System. The detector configuration and image interpolation algorithms are specific to this manufacturer therefore our results are valid only on this scan and cannot be extended to another one.

In addition, we performed the four acquisition protocols at the equilibrium phase of the liver. In this phase, contrast material enhancement of the liver (and therefore contrast to noise ratio) is decreased compared to scan after a 60 s delay, which is used in clinical routine. Consequently, the increased image noise when using thin collimations may be less relevant in images obtained after a scan delay of 60 s due to the higher contrast to noise ratio.

In conclusion, we found that MDCT using thin section of 2.5 mm or an increased table speed is less efficient in detecting low-contrast lesion in the liver (Table 1).

Table 1 Acquisition protocols comparison

Protocols	Slice thickness (mm)	Table speed (mm/rotation)	Pitch
1	5	30	1.5
2	5	15	0.75
3	5	11.25	0.75
4	2.5	15	1.5

Acknowledgements This article is dedicated to the memory of Yasmine Abdelmoumene MD.

References

1. Roos JE, Desbiolles LM, Willmann JK, Weishaupt D, Marincek B, Hilfiker PR (2002) Multidetector-row helical CT: analysis of time management and workflow. Eur Radiol 12:680–685
2. Sugarbaker PH (1990) Surgical decision making for large bowel cancer metastatic to the liver. Radiology 174:621–626
3. Nakamura S, Suzuki S, Baba S (1997) Resection of liver metastases of colorectal carcinoma. World J Surg 21:741–747
4. Prokop M (2003) Multislice CT: technical principles and future trends. Eur Radiol Suppl 5:M3–M13
5. Itoh S, Ikeda M, Achiwa M, Ota T, Satake H, Ishigaki T (2003) Multiphase contrast-enhanced CT of the liver with a multislice CT scanner. Eur Radiol 13:1085–1094
6. Valls C, Andia E, Sanchez A et al. (2001) Hepatic metastases from colorectal cancer: preoperative detection and assessment of resectability with helical CT. Radiology 218:55–60
7. Schmidt J, Strotzer M, Fraunhofer S, Boedeker H, Zirngibl H (2000) Intraoperative ultrasonography versus helical computed tomography and computed tomography with arterioportography in diagnosing colorectal liver metastases: lesion-by-lesion analysis. World J Surg 24:43–47
8. Kuszyk BS, Bluemke DA, Urban BA et al. (1996) Portal-phase contrast-enhanced helical CT for the detection of malignant hepatic tumors: sensitivity based on comparison with intraoperative and pathologic findings. Am J Roentgenol 166:91–95
9. Fleischmann D (2003) Use of high-concentration contrast media in multiple-detector-row CT: principles and rationale. Eur Radiol Suppl 5:M14–M20
10. Schoellnast H, Tillich M (2004) Improvement of parenchymal and vascular enhancement using saline flush and power injection for multiple-detector-row abdominal CT. Eur Radiol 14:659–664
11. Verdun FR, Denys A, Valley JF, Schnyder P, Meuli RA (2002) Detection of low-contrast objects: experimental comparison of single- and multi-detector row CT with a phantom. Radiology 223:426–431
12. Therasse P, Arbuck SG, Eisenhauer EA et al. (2000) New guidelines to evaluate the response to treatment in solid tumors. European Organization for Research and Treatment of Cancer, National Cancer Institute of the United States, National Cancer Institute of Canada. J Natl Cancer Inst 92:205–216
13. Jones E, Chezmar J, Nelson R, Bernardino M (1992) The frequency and significance of small (less than or equal to 15 mm) hepatic lesions detected by CT. Am J Roentgenol 158:535–539
14. Schwartz LH, Gandras EJ, Colangelo SM, Ercolani MC, Panice DM (1999) Prevalence and importance of small hepatic lesions found at CT in patients with cancer. Radiology 210:71–74
15. Valette PJ, Pilleul F, Crombe-Ternamian A (2003) MDCT of benign liver tumors and metastases. Eur Radiol Suppl 5:M31–M41
16. Marchiano A (2003) MDCT of primary liver malignancies. Eur Radiol Suppl 5: M26–M30
17. Commission of the European Communities (2000) European guidelines on quality criteria for computed tomography. EUR 16262 EN Luxembourg, Belgium: European Communities
18. Kalra MK, Maher MM, Saini S (2003) Multislice CT: update on radiation and screening. Eur Radiol 13:M129–M133
19. Verdun FR, Lepori D, Monnin P, Valley JF, Schnyder P, Gudinchet F (2004) Management of patient dose and image noise in routine pediatric CT abdominal examinations. Eur Radiol 14 835–841
20. Hormann M, Philipp MO, Eberl H et al. (2004) The effect of varying low-dose protocols on perceived image quality in multidetector CT in a rabbit model of acute appendicitis. Eur Radiol 14:1465–1471
21. Greess H, Lutze J, Nomayr A et al. (2004) Dose reduction in subsecond multislice spiral CT examination of children by online tube current modulation. Eur Radiol 14:995–999
22. Hu H, He HD, Foley WD, Fox SH (2000) Four multidetector-row helical CT: image quality and volume coverage speed. Radiology 215:55–62
23. Fox SH, Toth T (2002) Dose reduction on GE CT scanners. Pediatr Radiol 32:718–723
24. Weg N, Scheer MR, Gabor MP (1998) Liver lesions: improved detection with dual-detector-array CT and routine 2.5-mm thin collimation. Radiology 209:417–426
25. McCollough CH, Zink FE (1999) Performance evaluation of a multi-slice CT system. Med Phys 26:2223–2230
26. Haider MA, Amitai MM, Rappaport DC (2002) Multi-detector row helical CT in preoperative assessment of small (< or =1.5 cm) liver metastases: is thinner collimation better? Radiology 225:137–142
27. Polacin A, Kalender WA, Marchal G (1992) Evaluation of section sensitivity profiles and image noise in spiral CT. Radiology 185:29–35
28. Wilting JE, Timmer J (1999) Artefacts in spiral-CT images and their relation to pitch and subject morphology. Eur Radiol 9:316–322
29. Fleischmann D, Rubin GD, Paik DS et al. (2000) Stair-step artifacts with single versus multiple detector-row helical CT. Radiology 216:185–196